# Far-Infrared Interferometry from Antarctica

Hiroshi Matsuo
*Advanced Technology Center, National Astronomical Observatory of Japan, Mitaka, Tokyo 181-8588, Japan*
Contact: h.matsuo@nao.ac.jp, phone +81-422-34 3915

***Abstract*— Future high-angular resolution far-infrared interferometers and their possible implementation plans on high altitude sites such as Dome Fuji or Dome A in Antarctica is presented. Importance of observing far-infrared atomic fine-structure lines is discussed referring to recent *AKARI* observations of a high mass star-forming region.**

## I. Introduction

Astronomy in terahertz frequency region is advancing rapidly owing to the development of detector technologies, large aperture telescopes on high mountains and cryogenic telescopes in space. Variety of astronomical sources is probed in this frequency range by molecular and atomic lines and dust continuum emissions. Those are also important probes of distant galaxies as well as the Sunyaev-Zel'dovich effects for distant galaxy cluster searches.

In far-infrared region, Japanese satellite *AKARI* has made all sky survey in six bands [1]. A Fourier transform spectrometer was installed in the far-infrared surveyor (FTS/FIS) which made imaging spectroscopic observations [2]. Here, an observation of interstellar material around a massive star, Eta Carinae is presented as an example.

To study more detail of the source distribution or observe distant objects, higher angular resolution observations by space-based far-infrared interferometer is needed, but this required technology developments of detectors and interferometers. In this paper I discuss on far-infrared interferometry from high altitude plateau in Antarctica. I will compare the performance of heterodyne and direct detector interferometers and show that direct detector interferometers can achieve wide-field and high angular resolution imaging.

As an example of direct detector interferometry, experimental performance of a double input Martin-Puplett type interferometer that realized multiplying interferometer is reviewed in the last section.

## II. Probes of Distant Universe

Here I'd like to summarize astronomical probes of distant universe. Following three components are important in millimetre, submillimeter and far-infrared astronomy.

- Interstellar dust in starburst galaxies observed by thermal emission.
- Hot plasma in galaxy clusters observed by Sunyaev-Zel'dovich effects.
- Photo-dissociation and ionized regions observed by atomic fine-structure lines.

Firstly, high-redshift starburst galaxies are observed by wide field surveys. One example is millimetre-wave survey by AzTEC bolometer array on ASTE telescope toward *AKARI* deep field south [3]. Because of its large negative K-correction, millimetre-wave observations selectively sampled galaxies at high redshifts.

Secondly, Sunyaev-Zel'dovich effects have been a probe to measure the Hubble constant and also to identify thermal structure of the plasma [4]. Because Sunyaev-Zel'dovich effects are interaction of hot plasma with cosmic background radiation, the intensity does not decline as a function of redshift.

Thirdly, far-infrared atomic forbidden emission lines play an important role as coolants of PDRs and HII regions. The emission could be probes of starburst activities of high-redshift universe. But, we still do not understand into detail the physical conditions each atomic line probes, mostly due to the limited imaging capabilities and angular resolutions.

The following figure illustrate the importance of observing in terahertz frequencies, where variety of emission can be observed as distortion of background or as foreground emission in Wien part of the cosmic background radiation in all the redshift range. This frequency region can be called as 'Terahertz Cosmic Window' to the distant universe.

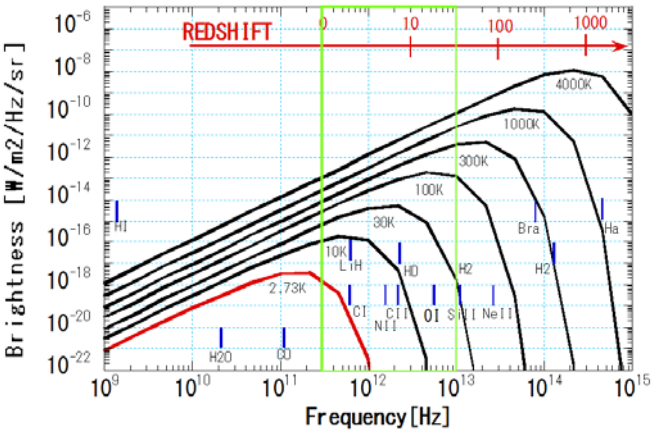


Fig. 1 The Terahertz Cosmic Window.

## III. FIR Lines of Interests

There are a number of far-infrared forbidden transition lines from ionized and neutral atomic species such as [OI] 63 μm, 145 μm, [OIII] 52 μm, 88 μm, [NII] 122 μm, 205 μm and [CII] 158 μm. These lines are major coolants of photo-dissociation and ionized regions [5]. To postulate importance

of atomic fine structure line, I present *AKARI* observation of interstellar material around one of the most massive star in our galaxy, Eta Carinae [6]. It is known that Eta Carinae is a binary with the primary Luminous Blue Variable with mass of about 100 $M_\odot$ and a companion of 30 $M_\odot$, both with violent mass loss activities [7]. Distance to the star is only 2.3 kpc and extinction toward the star and Carinae Nebula is small and detailed studies have been made by optical emission lines [8]. Studies of interstellar environments of the most massive stars in local universe are also linked to the understanding environments of massive stars in the early universe, Pop III stars.

### *A. Observations with AKARI*

Seven pointed observation was made using FTS/FIS in 2007. Observational details, data reduction and analysis is given in [6, 9]. Figure 1(a) and (b) shows the distribution of [CII] 158 μm and [OIII] 88 μm lines around Eta Carinae. Referring to the Hα emission in figure 1(c), west from Eta Carinae with ionized emission and molecular gas in front is called the Keyhole Nebula. The head of the Keyhole Nebula, with the arc-like emission that is aligned with the stellar wind axis, is thought to be related to the past activity of Eta Carinae [9].

The [CII] emission seems to peak around the head of the Keyhole where ionized nitrogen line [NII] 122 μm is also observed. Toward the opposite side of the stellar wind axis to the south-east, [CII] emission is also observed. In this region there is no indication of ionized gas, but the area is where stellar wind interacts with molecular clouds. The apparent alignment of the [CII] emission peaks seems to indicate that it is related to the past stellar wind activities. The current mass loss rate of Eta Carinae is estimated to be $10^{-4}$ - $10^{-3}$ $M_\odot$ /yr with velocity of about 600 km/s. Assuming the same velocity it takes about 5000 year for the stellar wind to interact with the ionized region or molecular clouds, which are 3-5 pc away from Eta Carinae

The [OIII] emission, on the other hand, has strong emission to the west of Eta Carinae. Intensity of the [OIII] emission is more than ten times stronger than [CII] emission peak at Keyhole and strong EUV ionization source is required to ionize oxygen with ionization potential of 35 eV. The strong [OIII] emission come from the edge of ionized arc and the clump 4 or the feature called defiant finger [10]. From analysis of optical emission lines, ionization sources of the region are thought to be W25 and O4 If-type star Tr16-244 that are at the south-west corner of Hα image in figure 2(c). Since critical density of [OIII] 88 μm is $5\times10^2$ $cm^{-3}$, it can be efficient coolant of low density ionized gas. Combination with [OIII] 52 μm emission with different critical density can be used to estimate density of the ionized gas.

### *B. Requirements to Future Observations*

Far-infrared spectroscopic observations by *AKARI* FTS/FIS revealed some physical condition of interstellar material around a massive star, which shows variety of activities related to the stellar activities and highly ionizing UV flux within the region. To identify the physical condition and comparing with observation at other wavelength region, it is important to make higher angular resolution observations. Higher angular resolution observations by Herschel Space Observatory will provide more details of ionization and density structure.

The Carina Nebula is the nearest high mass star-forming region where we can observe into detail. To conduct observation in other star-forming regions and also in nearby galaxies, still higher angular resolution observations are required. Space based far-infrared interferemetry will be the next step, but developments of detector and interferometer technologies are still on the way. In the next section I discuss what we can start in a short time scale to realize far-infrared interferometry on Antarctica Plateau.

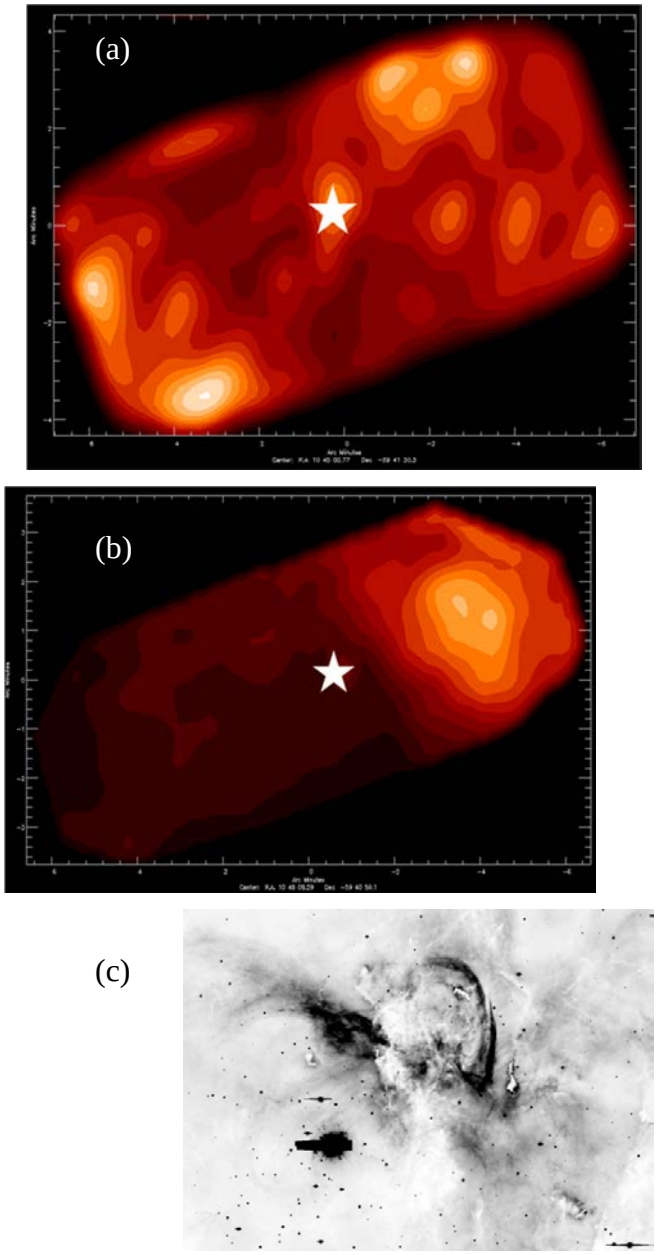


Fig. 2 Eta Carina and its surroundings observed by *AKARI*. (a) [CII] 158 μm, (b) [OIII] 88 μm, and (c) Hα image by Smith et al. (2002) as a reference to the Keyhole Nebula. Coordinates are R.A.-Dec, and scale is identical.

## IV. Antarctic Terahertz Interferometer

Observing condition of terahertz frequencies in Antarctica, sensitivity requirements and realization method will be discussed.

### A. Atmospheric Transmission

Since terahertz radiation is absorbed by water vapour, high altitude site and/or cold sites are preferred for astronomical observations in millimetre and submillimeter-waves, such as Hawaii, Atacama and South Pole in Antarctica. High plateaus in Antarctica, such as Dome A or Dome Fuji, will be the ultimate site for astronomical observations, and that are unique sites for terahertz astronomy from ground.

Figure 3 shows calculated atmospheric transmission from high altitude site in Antarctica using 'am' program [11] assuming precipitable water vapour of 75 μm.

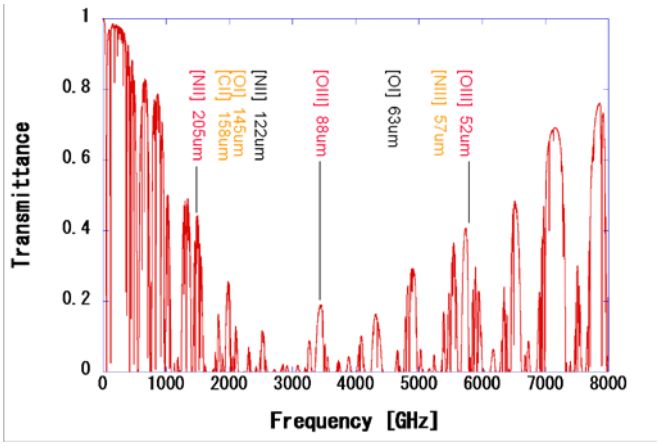


Fig. 3 Atmospheric transmission calculated for 75 μm precipitable water vapour from 4100 m altitude in Antarctica using 'am' program [11].

Under this condition, some fine structure atomic lines can be observed through atmospheric windows at terahertz frequencies. [NII] 205 μm have been observed by the SPIFI instrument at South Pole [12]. Doubly ionized oxygen lines, [OIII] 52μm and 88 μm, could be observed with a transparency of better than 10% whereas [CII] 158 μm, [OI] 145 μm and [NIII] 57 μm with lower transparencies from high plateau in Antarctica.

### B. Sensitivity of THz interferometers

First I compare heterodyne and direct detector interferometry. For ground based observations, sensitivity of heterodyne and direct detector interferometry is almost identical if the observing system is background and quantum noise limited. However, under low background condition in millimetre-wave or at high frequencies more than a few THz direct detector observations can be more sensitive. In terms of observing bandwidth, atmospheric windows will limit observing bandwidth up to several 10 GHz.

Heterodyne interferometry is a matured technology and many telescope apertures can be combined to make large arrays. On the other hand, direct detector interferometry is still under development and telescopes have to be optically connected and the number of antennas is limited.

TABLE I
Sensitivity of Terahertz Interferometers

| | Direct detectors | Heterodyne |
|---|---|---|
| Aperture diameter | 1 m | 1 m |
| Element number | 2 | 10 |
| Base line | 50 m | 50 m |
| Wavelength | 200 μm | 200 μm |
| NEP/η or $T_{sys}$ | $10^{-15}$ W/Hz$^{0.5}$ | 500 K |
| Bandwidth | 10 GHz | 10 GHz |
| Focal plane array | 1000 | 1 |
| Synthesized beam | 1 " | 1 " |
| Field of view | 0.25 deg$^2$ | 0.5 arcmin$^2$ |
| NEFD | 20 mJy (1σ, 12h) | 10 mJy (1σ, 12h) |

The bandwidths can be wider for direct detectors and narrower for heterodyne detectors. For continuum study wider bandwidth is advantageous but background limited NEP will be degraded. For spectroscopic observations, heterodynes are advantageous for their high frequency resolution, but direct detector sensitivity also improves by limiting observing bandwidth.

Field of view would be a large factor in favour of direct detector interferometry. Current technologies enable focal plan array of more than 1000 elements. Signals from the direct detector interferometers can be sampled relatively slowly, and data recording systems are not limiting factors. On the other hand heterodyne interferometer required fast sampling and processing is required that limit number of detectors, hence the observing field of view.

### C. Configuration

Direct detector interferometry requires input aperture mirrors and a beam combiner. Simplest configuration will be like figure 4(a). Aperture mirror can be on a straight boom or on a round track as shown in the figure. Mirrors on the track reflect signal from astronomical sources to a beam combiner at the center. For installation in high plateau in Antarctica it is better to make the interferometer as simple as possible. All components except a round track can be compact with sizes of about 1 m. To make beam combiner compact, beam diameter at combiner should be decreased to about 100 mm, which should also accommodate with focal plane detector arrays.

Figure 4(b) shows possible configurations of the four-beam interferometer. One Martin-Puplett type beam combiner that uses wire grid can make interferograms from linearly polarized signal. Four beam combiners can make use of dual polarization beams from four input mirrors. For compensation of different optical path between two sets of mirrors, optical delay should be implemented that is schematically shown in figure 4(b) at the bottom.

Since Martin-Puplett interferometer is polarizing interferometer, combination of polarizer angles gives measurements of different polarization state; parallel combination gives measurements of I and Q, orthogonal combination for U and V.

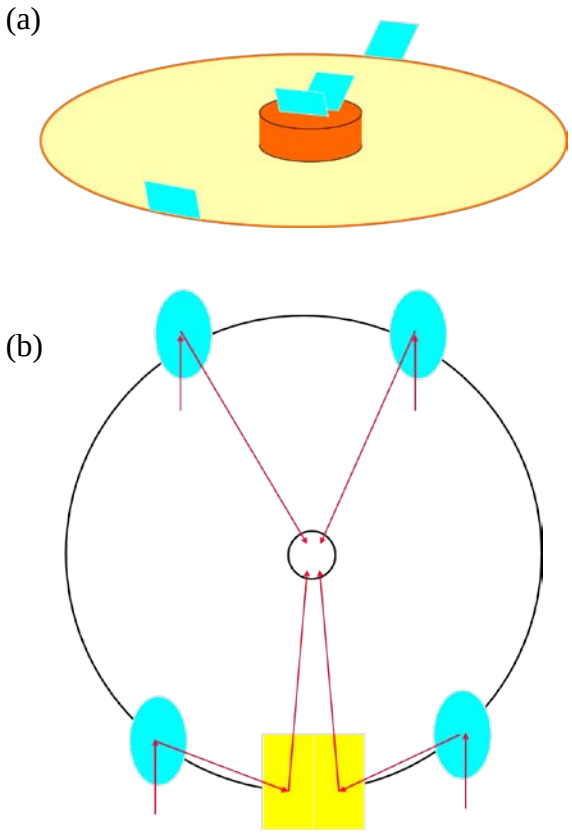


Fig. 4 Possible configurations of far-infrared interferometers. Top figure shows two-element interferometer on a round track. A beam combiner is at the center. Bottom figure shows four-element interferometer. There is additional delay line compensation optics.

### *D. Technology developments*

There are two types of millimetre and submillimeter-wave bolometric interferometers under study. One uses a Fizeau type interferometer [13] and another used Michelson type interferometer [14, 15]. Here I review the performance of a Michelson type, especially the one using wiregrid as beam combiner, which is called as Martin-Puplett type interferometers.

Martin-Puplett type Fourier transform spectrometers have been used for wide band measurements in millimetre and submillimeter-waves [16]. To measure spectra of sources, both input and output polarizers are used. Poloarity of output signal depends on the configuration of the input and output polarizers. By subtracting parallel configuration signal from that of orthogonal, DC component and common fluctuations are subtracted. This is very useful for two aperture interferometer, since this subtract all common fluctuation such as atmospheric fluctuation. This is the merit of multiplying type interferometer realized by Martin-Puplett type bolometric interferometers. Experimantal demonstration was made in [17, 18] by measuring interferogram of the moon in millimetre-wave. Figure 6 shows the measured interferogram and its Fourier transformation that clearly shows atmospheric fluctuation is subtracted by measuring two output ports of the Martin-Puplett interferometer.

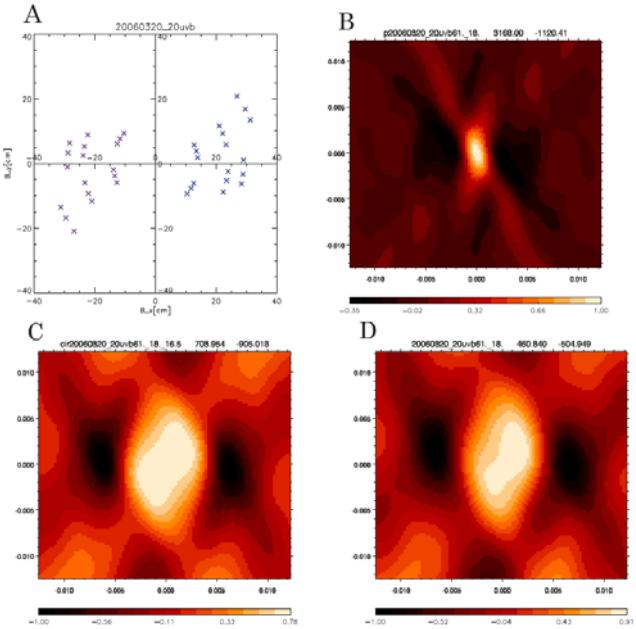


Fig. 5 Synthesized image of the sun by bolometric interferometer [17, 18]. Measurement was made with 5 cm aperture and 35 cm baseline, and 150-350 GHz frequency range was used for image reconstruction. Ge composite bolometer at 1.5 K is used for observation. A: baseline coverage, B: synthesized beam, C: simulated image, D: synthesized image of the sun.

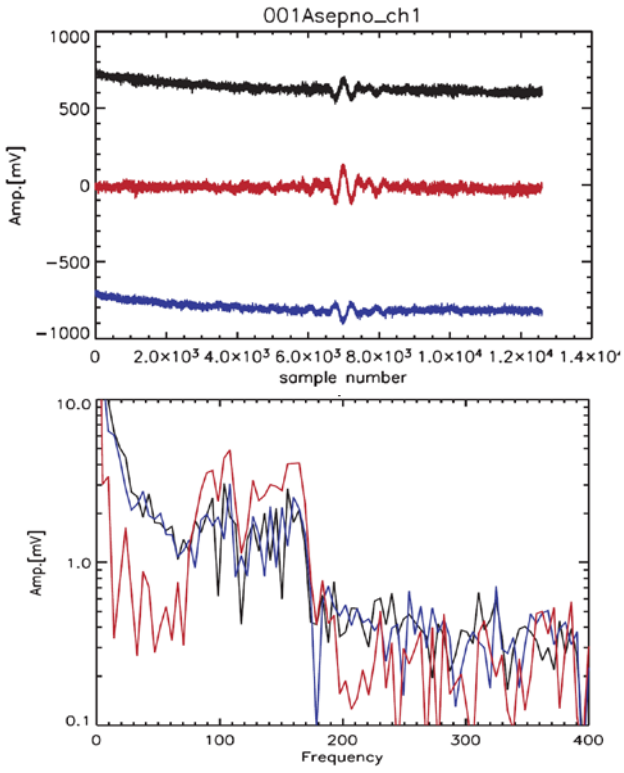


Fig. 6 Demonstration of multiplying interferometer by observing the moon [17, 18]. Top figure shows interferograms at two output ports in black and blue, and subtracted interferogram in red. Bottom figure shows Fourier transformation of the interferograms. The output signal in red clearly shows that atmospheric fluctuation is cancelled.

## V. Conclusions

Results on far-infrared observations of a massive star-forming region by *AKARI* show a complex nature of interstellar material. For more detailed study of the region or observing massive star-forming region in nearby galaxies, higher angular resolution capability is required. Interferometry on a high plateau in Antarctica offers opportunities for high angular resolution observations in the far-infrared using either heterodyne or direct detectors. Direct detector interferometers can be more sensitive and achieve wider field of view than heterodyne system. Performance of a Martin-Puplett type double input interferometer was reviewed that can subtract common fluctuations of atmospheric emission.

## Acknowledgment

Part of this research is based on observations with *AKARI*, a JAXA project with the participation of ESA. HM thank Scott Paine of Harvard Smithonian Center for Astrophysics for supplying atmospheric model over Antarctica.

## References

[1] H. Murakami et al., "The Infrared Astronomical Mission AKARI", PASJ 59, S369-S376 (2007)

[2] M. Kawada, H. Takahashi, N. Murakami, H. Matsuo et al., "Performance of an Imaging Fourier Transform Spectrometer with Photoconductive Detector Arrays: An Application for the AKARI Far-Infrared Instrument", PASJ 60, S389-S397 (2008)

[3] B. Hatsukade, K. Kohno, Y. Tamura et al. "AzTEC/ASTE Deep Survey: 1.1-mm Map and Source Catalogue of the AKARI Deep Field South and Number Counts", in preparation

[4] E. Komatsu, H. Matsuo, T. Kitayama, M. Hattori et al., "Substructures Revealed by the Sunyaev-Zel'dovich Effect at 150 GHz in the High Resolution Map of RX J1347-1145", PASJ 53, 57-62 (2001)

[5] A.G.G.M. Tielens, "The Physics and Chemistry of the Interstellar Medium", Cambridge University Press (2005)

[6] H. Matsuo, A. Kosaka, T. Arai, N. Nitta, "Far-Infrared Spectroscopic Imaging of Interstellar Material around Eta Carinae", ASP Conference Series, Vol. 418, pp. 451-454 (2009)

[7] A. Okazaki, S.P. Owocki, C.M.P. Russell, M.F. Corcoran, "Modelling the *RXTE* light curve of η Carinae from a 3D SPH simulation of its binarywind collision", MNRAS 388, L39-L43 (2008)

[8] N. Smith, "Near-infrared and optical emission-line structure of the Keyhole Nebula in NGC 3372", MNRAS 331, 7-12 (2002)

[9] H. Matsuo, A. Kosaka, T. Arai, N. Nitta, M. Tanaka, "Far-Infrared Spectroscopic Imaging of Interstellar Material around Eta Carinae", in preparation

[10] N. Smith, R.H. Barba, N.R. Walborn, "Carina's defiant Finger: HST observations of a photoevaporation globule in NGC 3372", MNRAS 351, 1157-1470 (2004)

[11] S. Paine, "The *am* Atmospheric Model", SMA Technical Memo #152-Revision 3 (2004), http://www.cfa.harvard.edu/sma/memos/152-03.pdf

[12] T.E. Oberst, S.C. Parshley, G.J. Stacey, T. Nikola et al., "Detection of the 205 μm [NII] line from the Carina Nebula", ApJ 652, L125-L128 (2006)

[13] G.S. Tucker, J. Kim, P. Timbie, S. Ali, L. Piccirillo, C. Calderon, "Bolometric interferometry: the millimeter-wave bolometric interferometer", New Astronomy Reviews 47, 1173-1176 (2003)

[14] I.S. Ohta, M. Hattori, H. Matsuo, "Development of multi-Fourier transform interferometer: fundamentals", Applied Optics 45, 2576-2585 (2006)

[15] I.S. Ohta, M. Hattori, H. Matsuo, "Development of multi-Fourier transform interferometer: imaging experiment: imaging experiments in millimeter and submillimeter waveband", Applied Optics 46, 2881-2892 (2007)

[16] D.H. Martin, E. Puplett, "Polarized interferometric spectrometry for the millimetre and submillimetre spectrum", Infrared Physics 10, 105-109 (1969)

[17] I.S. Ohta, M. Hattori, Y. Chinone, Y. Luo, Y. Hamaji, J. Takahashi, H. Matsuo, N. Kuno, "Astronomical testing observation in Multi-Fourier transform interferometer: Aperture synthesis technique and CMB", Conference Digest of IRMMW-THz 2007, 335-336 (2007)

[18] Y. Luo, M. Hattori, I. S. Ohta, Y. Chinone, J. Takahashi, Y. Hamaji, H. Matsuo, N. Kuno, "Realization of multiplying type interferometer with 2-elements 0.3K bolometer detectors", IEEE conference proceedings, Global Symposium on Millimeter Waves, 213-215 (2008)